Oxygen-Free Production—From Vision to Application

Lienhard Wegewitz,* Wolfgang Maus-Friedrichs, René Gustus, Hans Jürgen Maier, and Sebastian Herbst

As oxygen negatively affects most production processes in the metalworking industry, a truly oxygen-free production environment appears attractive in terms of the resulting material and component properties. This overview summarizes research conducted within the Collaborative Research Centre (CRC) 1368. The objectives of this CRC are twofold. First, a fundamental understanding of the mechanisms that govern the interaction between a metal surface and the environment is established. Second, it is researched how this understanding can be exploited to improve current production processes and even develop completely new ones. Herein, data obtained within the first funding period, which already demonstrate that significant effects can be realized in processes such as thermal spraying, cold rolling, compound casting, laser brazing, milling or hot stamping to name just a few examples, are presented. In addition, key aspects such as initial deoxidation of the workpieces, their transport under conditions that prevent reoxidation, and the tools needed to establish and control an oxygen-free process environment are given, and the ramifications with respect to actual applications are discussed.

1. Introduction

Considering their historical development, the production processes of the metalworking industry were usually carried out in the presence of oxygen, i.e., in ambient air atmosphere. This causes oxidation of the metal surfaces, which results in oxide layers of varying thickness depending on the process temperature and the reactivity of the metal. Except for the positive effect for application due to the built-up of thin, dense oxide layers, so-called passivation layers, which offer corrosion protection and maintain this effect in the event of damage due to post-

L. Wegewitz, W. Maus-Friedrichs, R. Gustus
Clausthal Centre for Materials Technology
Clausthal University of Technology
Leibnizstraße 9, 38678 Clausthal-Zellerfeld, Germany
E-mail: lienhard.wegewitz@tu-clausthal.de

H. J. Maier, S. Herbst
Institut für Werkstoffkunde (Materials Science)
Leibniz Universität Hannover
An der Universität 2, 30823 Garbsen, Germany

The ORCID identification number(s) for the author(s) of this article can be found under https://doi.org/10.1002/adem.202201819.

oxidation (as is the case with high-alloy CrNi steels),[1] oxidation predominantly acts as a disturbing factor. Examples include the inhibition of wetting in brazing applications,[2] oxidation and during heat treatments,[3] or the acceleration of crack growth during material fatigue experiments.[4] For some processes, especially thermal ones, attempts are therefore made to reduce the oxygen concentration in the surrounding atmosphere by using inert gases or by moving the process to a vacuum chamber.[5–8] However, in conventional high-quality (5.0) inert gas atmospheres, oxygen concentrations in excess of 5 ppmv are present. Even in technical high vacuum (10^{-6} to 10^{-10} bar), component surfaces are still hit by oxygen molecules at a rate of well over one trillion (10^{12}) impacts per cm^2 each second. Under such conditions, metal surfaces are therefore quickly covered with an oxide layer.[3,9] The known possibilities of metal processing are thus considerably limited. Even ultrahigh vacuum (UHV) is far from sufficient for maintaining oxide layer-free metal surfaces for prolonged timespans.[10] Moreover, the technology for generating a UHV is complicated and correspondingly expensive. Thus, an implementation in actual production processes is often considered to be highly uneconomical, and thus rarely feasible on a large scale.

The potential of the technical possibilities inhibited by the presence of oxygen, which has been taken for granted until today, and the limits that exist in metal processing as a result affect almost all production processes. It is reasonable to assume that production processes in an atmosphere with oxygen partial pressures lowered by several orders of magnitude compared to conventional technologies would be able to offer considerable technical, economic, and resource-relevant advantages and provided that this atmosphere can be implemented in a technically simple and inexpensive manner. Completely new processes, which are so far unthinkable in the presence of oxygen, and the associated oxide layers can emerge utilizing such an atmosphere.

In order to use such an environment in actual technical processes, economic aspects for creating such an environment certainly play a key role. One promising approach to generating a practically oxygen-free environment at ambient pressure at low cost is the addition of small amounts of monosilane (SiH_4, hereinafter referred to as "silane") to inert gas atmospheres (argon, nitrogen, or, for special applications, helium).[11,12] By adding monosilane, the residual oxygen content present in the

inert gas atmosphere (usually <20 ppmv) is completely removed by conversion to SiO_2, H_2, and H_2O. Since the silane concentration only needs to be as high as the concentration of residual oxygen in the inert gas, even very small amounts of silane are sufficient. Thus, it can then be supplied in an already highly prediluted state, such that handling of the silane is not critical. The reaction starts already at room temperature and reduces the residual oxygen to below the detection limit. With regard to the presence of oxygen molecules, atmospheres corresponding to an extremely high vacuum (XHV) can thus be generated as depicted in **Figure 1**.
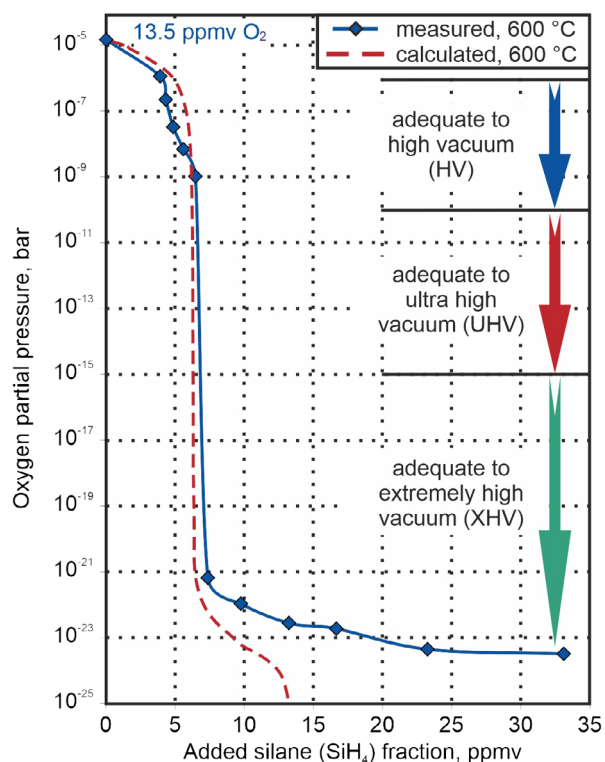
In the present context, we define kinetically oxygen-free atmospheres as atmospheres with oxygen partial pressures below 10^{-13} mbar as reoxidation is then negligible within typical processing times. This value is an approximation based on the oxide coverage of less than one percent of a monolayer on a surface in 10 h assuming a sticking coefficient of 1 because the first monolayer determines most chemical and thermodynamical processes. Of course, tolerable oxygen partial pressures depend on process and material, and thus need to be calculated for each application separately. For example, the reoxidation of the topmost layer for titanium surfaces in ambient air atmosphere is completed in several nanoseconds, whereas the time scale of cutting processes such as milling is in the range of microseconds or rather milliseconds.

Apart from high-temperature brazing processes, the approach of relocating production processes or their active zones to

XHV-adequate oxygen-free atmospheres represents a comparatively young field of research. Many of the results described in this work originate from the Collaborative Research Centre (CRC) 1368 "oxygen-free production." The CRC aims at applying the inexpensive and technically simple oxygen-free atmosphere to a wide range of production processes, starting with an understanding of the mechanisms in the active zone and working toward process understanding and complete process chains in oxygen-free atmosphere.

By applying the oxygen-free environment to a wide range of production fields, several potentials can be exploited: 1) The use of starting materials that are free of oxide layers and do not reoxidize during the process leads to an improved material bonding between these materials, and thus offers a wide range of options in terms of their type and shape and in terms of the components that can be manufactured with them. 2) Production of semi-finished products and components with completely new property profiles through the joining of previously not joinable material systems and the application of new production processes. 3) Use of novel tool material systems that cannot currently be used due to their high oxidation tendency, but which have unique properties. This applies to both substrates and coatings. 4) Increased energy and material efficiency of production processes by eliminating tribooxidation as a wear mechanism and reducing process forces required to break up oxide layers. In addition, the reduction of process temperatures in thermal joining and coating processes and the elimination of wetting-promoting, scaling-preventing, and covering additives (fluxes, welding slag powders) can be expected.

In order to produce oxide layer-free surfaces and compounds or to avoid the incorporation of oxide layer-induced defects in interfaces, depending on the process conditions, either the absence of oxygen is already sufficient in thermal processes and in the creation of new surfaces by machining or forming, or active deoxidation must be added upstream of the respective process. In the processes considered, the oxides are therefore removed mechanically (e.g., by machining operations), thermally (e.g., by laser or plasma arc) or plasma-chemically in a nonthermal plasma. Kinetically, the formation of new oxide layers in an oxygen-free environment is excluded due to the extremely low oxygen partial pressure (cf. Figure 1), even with long process times.

2. Methods and Technology

2.1. Generation of Oxygen-Free Atmospheres

The idea of generating oxygen-free atmospheres using silane is based on the high reactivity of silane, especially monosilane (SiH_4), toward molecular oxygen. According to Equation (1) and (2), monosilane reacts with oxygen to form silicon dioxide (SiO_2) and hydrogen (H_2), respectively, water (H_2O)

$$SiH_4(g) + O_2(g) \leftrightarrow SiO_2(s) + 2H_2(g) \tag{1}$$

$$SiH_4(g) + 2O_2(g) \leftrightarrow SiO_2(s) + 2H_2O(g) \tag{2}$$

The reaction between silane and oxygen is highly exothermic and takes place already at room temperature. Silane is used
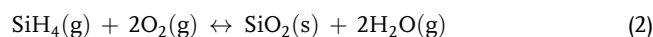

Figure 1. Extreme reduction of the oxygen concentration in a technical nitrogen atmosphere (13.5 ppmv initial oxygen content) at room temperature by silane doping. Adapted with permission[78] Copyright 2014, Springer.

particularly in the semiconductor industry as a precursor for the preparation of silicon and silicon dioxide thin films. In oxygen-free production, silane is used as an oxygen scavenger, eliminating nearly all residual oxygen in the process atmosphere. As an oxygen content of 10^{-17} ppm can be achieved. For comparison, even commercially available inert gases like argon 5.0 or nitrogen 5.0 still contain at least about 1-2 ppm oxygen as residual contamination. This amount of contamination is sufficient to cover the surface with oxygen within milliseconds.

In order to generate oxygen-free atmospheres, silane has only to be added in the order of magnitude as oxygen is present, cf. Equation (1). To minimize the silane required and the silica formed during the reaction, it is reasonable to use inert gases like argon or nitrogen as the starting atmosphere. As a consequence, highly diluted, and thus harmless silane-doped inert gas mixtures can be applied. In the CRC, the experiments on oxygen-free production are primarily carried out in commercially available glove boxes filled with argon 5.0 (purity: 99.999%). For safety reasons, the silane is then added as an argon/silane mixture with a silane content of only 1.5% (Linde GmbH). In order to reduce the amount of silane required for eliminating the residual oxygen, the glove boxes are flushed several times with pure argon until the oxygen content in the atmosphere cannot be reduced further. Due to the high volume and the large surfaces within the glove boxes, the oxygen content in the glove box atmosphere measured by an oxygen sensor is usually significantly higher than for pure argon 5.0. However, multiple flushes can typically reduce the oxygen content within the glove box to less than 100 ppm.

Considering a glove box with a volume of 1 m³ and an oxygen content of 100 ppm, this amounts to an oxygen partial volume of 1×10^{-4} m³. From Equation (1), one silane molecule can eliminate one oxygen molecule. In a first approximation, 1×10^{-4} m³ silane should be necessary to eliminate the residual oxygen content in the glove box atmosphere. Considering a silane supply of 1.5% silane in argon, this amounts to an argon/silane gas volume of about 6.6×10^{-3} m³ or 0.66% of the glove box volume. In summary, only 0.66% of the glove box volume needs to be exchanged to eliminate 100 ppm residual oxygen. In general, the required silane mixture can be calculated as follows

$$V_{Ar+SiH_4} \approx \frac{100\%}{x_{SiH_4}} \cdot p_{O_2} \cdot 10^{-6} \cdot V_{glove\,box} \tag{3}$$

with V_{Ar+SiH_4} is the volume of the argon/silane gas mixture in m³, x_{SiH_4} is the fraction of silane in the argon/silane gas mixture in %, p_{O_2} is the amount of residual oxygen in ppm, and $V_{glove\,box}$ is the volume of the glove box in m³.

In order to avoid adding more silane than is actually necessary to eliminate the residual oxygen, the supply of silane should be controlled. This can be done by adding silane via gas flow regulators. **Figure 2** shows the oxygen content over time of the atmosphere of a glove box (0.4 m × 0.4 m × 0.7 m, prefilled with argon 5.0) to which small amounts of silane were continuously added. The silane was supplied by mixing argon 5.0 with silane-doped argon 5.0 (1.5% silane) using two independent gas flow regulators. The mixing ratio was 400:3, which results in a silane content of 112 ppm silane in argon. The silane/argon mixture
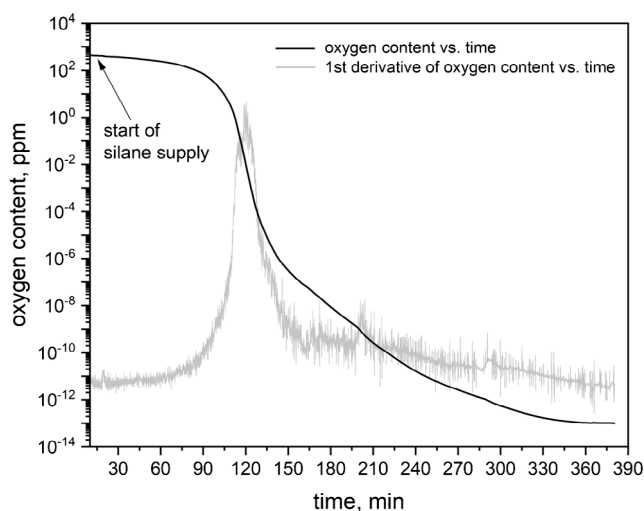
Figure 2. Oxygen content of an argon atmosphere as a function of time during continuous supply of silane in a custom glove box prefilled with argon 5.0[48]; the gray curve shows the first derivative of the oxygen content as an indicator of the change in oxygen concentration.

was introduced at a flow rate of approx. 0.4 L min^{-1}. The initial oxygen content within the glove box was about 400 ppm.

As Figure 2 shows, the continuous supply of silane initially leads to a continuous decrease in oxygen content, leading to a measured oxygen fraction of about 10^{-7} ppm after 150 min. In the next 210 min, the oxygen content decreases slowly and reaches a value of about 10^{-13} ppm. The rate of oxygen elimination depends primarily on the initial amount of oxygen present, the flow rate, the amount of silane added, and the oxygen leakage rates of the process chamber and feed lines. In addition, the size and construction of the process chamber (resp. glove box) can also influence the conversion rate. For instance, a circulating air fan can be used to accelerate the oxygen elimination in large and winding chambers. Care must be exercised to not use high concentrations of silane or flooding a glovebox with gases containing high oxygen partial pressures because these incidents can lead to precipitation of particles consisting of silicon and silicon dioxide.

2.2. Sensors for Monitoring Oxygen-Free Atmospheres

The determination of the oxygen partial pressure represents an important step in the process of generating oxygen-free atmospheres and oxygen-free production in general. By measuring the oxygen partial pressure before the production process, the amount of silane required to remove the residual oxygen can be estimated. Thus, the supply of silane can be adjusted according to the actual oxygen contamination. By measuring the oxygen partial pressure during the production process, in contrast, the oxygen-free conditions can be monitored and if necessary, countermeasures can be initiated on time.

To monitor oxygen in the gas phase, different kinds of sensor technologies are available. Depending on the measuring principle, common oxygen sensors can be divided in potentiometric, amperometric, resistive/conductive, magnetic and optical
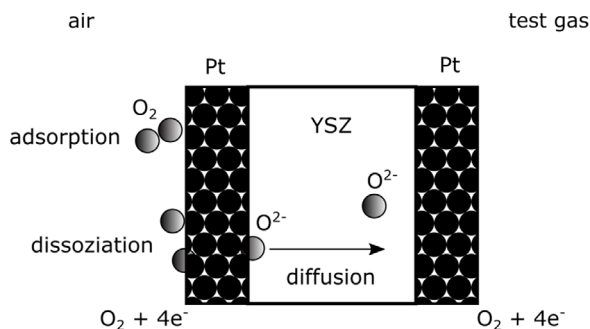
sensors.[13] In oxygen-free production, the oxygen sensor must meet certain requirements. The sensor should have no cross-sensitivities, should be low-maintenance, and fast enough to monitor rapid changes in oxygen concentration. However, the most important one concerns the required measuring range, which must cover several orders of magnitude, at least from 10^3 to 10^{-13} ppm.

In the CRC, solid-state potentiometric gas sensors are used to monitor the oxygen concentration. These sensors make use of the high oxygen ion conductivity of a solid electrolyte like yttria stabilized zirconia (YSZ) to measure the concentration difference between a reference and a working electrode.[14–16] The solid electrolyte is gas impermeable so that only oxygen ions can pass the gas-separating electrolyte. The ion conductivity of YSZ becomes significant at elevated temperatures and originates from oxide vacancies, which are formed by doping zirconia with yttrium. The electrodes of the sensor are usually made of porous platinum. Molecular oxygen adsorbed on the electrodes dissociates into atomic oxygen, which are reduced to O^{2-} ions at the triple-phase boundary (Pt-YSZ-gas) by electron transfer from the platinum electrode to the oxygen. In case of a concentration difference in oxygen activity (partial pressure) between the reference and the working electrode, oxygen ions diffuse through the solid electrolyte, creating a potential difference between the two electrodes. A schematic diagram of a solid electrolyte oxygen sensor based on YSZ is shown in **Figure 3**. The potential difference can be measured and is given by the Nernst equation

$$U = \frac{R}{4F} \cdot (T + T_{offset}) \cdot \ln\left(\frac{p_r}{p_w}\right) + U_{offset} \tag{4}$$

where U is the sensor voltage, R is the gas constant, T is the temperature, F is the Faraday constant, p_r is the partial pressure of oxygen at the reference electrode, and p_w is the partial pressure of oxygen at the working electrode. According to Equation (4), the sensitivity of the sensor depends, besides the oxygen partial pressures, only on the temperature T. As reference, a gas with well-known and constant concentration of oxygen should be used. The most common way is to use air as reference, which has an average oxygen concentration of 20.9 Vol% (depending on the relative humidity).

Solid state oxygen gas sensors offer a number of advantages: they are highly selective, offer long-term stability, and have a short response time. In addition, these sensors have a wide measurement range of several orders of magnitude, which make them ideal for measuring the oxygen concentration in the present case.

In the CRC, a solid-state oxygen sensor from MESA Mess- und Regeltechnik Vertriebs- und Service GmbH is used. The sensors are embedded in a metal housing with integrated temperature regulation and two ports for gas inlet and outlet. Each sensor is connected to a power supply unit containing a gas pump for gas extraction and a high precision power supply for the regulation and stabilization of the sensor heating. As reference for the oxygen measurement, ambient air is used. The sensors are heated up to 873 K during measurement and provide an output voltage between 0 and 1300 mV, which corresponds to an oxygen concentration range of 20.9 Vol% to about 10^{-26} Vol%.

The probe voltage can be read out, for example, using a commercially available multimeter. The actual oxygen content can then be calculated using Equation (4). However, to ensure an accurate measurement, the actual temperature of the sensor must be known exactly, which may vary slightly from sensor to sensor. Since the temperature cannot be measured directly, a test gas with well-known oxygen content, for example, 0.1% oxygen in argon, can be used to calculate the temperature offset T_{offset}. An additional voltage offset U_{offset} can be determined by measuring the sensor voltage using ambient air as test gas.

2.3. Deoxidation of Samples and Workpieces

Oxygen influences materials and processes in two ways—first by the oxygen content in the surrounding atmosphere and second due to oxygen incorporated in oxide layers. The first influence can be suppressed by the addition of silane to an inert gas atmosphere, as described in Section 2.1. To address the second one, the oxide layers have to be removed by a deoxidation process. Conventionally, grinding, blasting, or chemical treatments like the use of fluxes or acid cleaning are employed. For some applications, this is done in atmosphere or under protective gas, which may lead to less brittle or thinner oxide layers with changes in composition, but necessarily involves a certain degree of reoxidation due to residual oxygen. A complete and lasting removal of oxide layers is not possible under those circumstances. Examples of such applications are fluxes in brazing applications and metal inert gas or metal active gas welding. These have in common that the influence oxygen has on the process is strongly reduced but not excluded.

To get closer to an oxygen-free process environment, metal and alloy surfaces are often thermally deoxidized in ultrahigh vacuum (UHV), especially for research applications.[17,18] Another example is the somewhat unorthodox deoxidation by an electron beam, which is only productive for the deoxidation of small substrates and structures.[19]

A different option is deoxidation in thermal or nonthermal plasmas. For example, Behera et al. describe the thermal deoxidation of iron ore in a thermal hydrogen plasma[20] and Rains et al. the thermal plasma deoxidation of aluminum oxide particles.[21] In most cases where solid substrates are deoxidized in a plasma, the process happens at lower gas temperatures compared to the aforementioned thermal plasmas. Mostly,

Figure 3. Schematic diagram of a potentiometric oxygen sensor using yttria stabilized zirconia (YSZ) as solid electrolyte.

**ADVANCED
SCIENCE NEWS**

www.advancedsciencenews.com

**ADVANCED
ENGINEERING
MATERIALS**

www.aem-journal.com

low-pressure plasmas are used for deoxidation. The process atmospheres generally include one or several reducing gases like hydrogen, carbon monoxide, or methane. Examples include the deoxidation of AISI 316L steel in a microwave plasma at 1000 °C and 40 Pa of hydrogen,[22] deoxidation of bronze alloys,[23] or aluminum oxide[24] in low-pressure radio frequency plasmas in hydrogen or argon–hydrogen.

2.3.1. Deoxidation by Dielectric Barrier Discharges for Oxygen-Free Production

All of the aforementioned methods exhibit certain disadvantages. Thermal deoxidation or deoxidation in thermal plasmas at sufficient temperatures changes the metallurgical properties of the material beneath the oxide layer. Deoxidation by mechanical means, e.g., grinding, changes the surface topography and may lead to incorporation of foreign material. Chemical treatments like acid cleaning or Ca vapor deoxidation may lead to incorporation of hydrogen or other foreign materials. Deoxidation in UHV environments is extraordinarily expensive for production scale quantities. Using low pressure plasmas in industrial applications leads to a low volume of production due to their nature as these are typical batch processes.[25,26]

An attractive method for deoxidation of pure metals and alloys is the use of dielectric barrier discharges (DBDs). This approach provides several advantages like low energy input at the treated surface, working at atmospheric pressure, and thus with relatively simple and inexpensive equipment. DBDs are not limited to batch processing but also allow continuous production. For a description of principles, equipment and applications of DBDs the reader is referred to.[27–30]

Until now, most research regarding deoxidation of metal oxides by DBDs focuses on copper oxides.[31–34] A notable exception is the DBD deoxidation of NiO to Ni in argon–hydrogen for catalysis.[35]

The amount of native copper oxide, for example, can be reduced by 70% in a mixture of 2% hydrogen in argon within about 2 s, while 96% reduction is achieved after 10 s.[36] Mixtures of monosilane in argon are used by the majority of the oxygen-free production processes described in Section 3. Deoxidation of native copper oxide is achieved in a DBD in silane-doped argon, but the reduction fraction does not reach 90% contrary to argon–hydrogen mixtures.[34]

The deoxidation of pure metal and alloy surfaces in DBDs is a promising method for certain oxygen-free production processes, but research regarding the deoxidation of a wider variety of materials is essential. While DBDs have many advantages offsetting the problems of other deoxidation methods described earlier, the treatment of complex surface geometries poses a challenge not to be underestimated. Furthermore, reduction processes on the basis of ion sputtering, which takes place in some low pressure plasmas,[24] do not occur in DBDs. This may limit the deoxidation of some metals and their alloys.

2.3.2. Deoxidation of Powders

Besides solid workpieces, metal powders are used in several production processes like laser powder bed fusion (LPBF), thermal spraying, or die pressing with subsequent sintering. Powders consist of metal particles, which in general are covered by native oxide layers or oxygen-containing organic layers. In certain applications like thermal spraying in silane-doped atmospheres, the oxide layer is at least partially reduced in the process itself. For other applications, deoxidized powders are necessary.

Oxide-free particles can either be directly produced, e.g., silicon particles in a microwave plasma in an argon/hydrogen/silane atmosphere[37] or deoxidized by different methods. The most common one is temperature programmed reduction in hydrogen, which is applied for catalyst powders for example.[38]

A major part of the research regarding powder deoxidation is related to titanium alloys and intermetallic compounds. One of the reasons is the poor recyclability of Ti scrap due to oxygen impurities. Deoxidation methods include elevated temperatures in presence of calcium and magnesium compounds,[39,40] electrochemical deoxidation,[41] or radio frequency plasma deoxidation of Ti–6Al–4V particles with calcium.[42] Hafnium oxide[43] or tantalum oxide and niobium oxide[44] powders can be reduced by electro-deoxidation.

More complexity is added to the deoxidation process if powders are not treated in filling but rather in a gaseous bed, which prevents agglomeration and blind spots. The thermal reduction of iron oxides in a circulating fluidized bed in hydrogen is an example.[45] A relatively new approach to powder deoxidation is the combination of a fluidized bed reactor with a nonthermal DBD plasma.

2.3.3. Deoxidation Methods in Oxygen-Free Production Processes

Several of the production processes in oxygen-free atmosphere described in Section 3 use deoxidized samples or workpieces. In some cases, like hot stamping, laser beam brazing, thermal spraying, or cutting, oxide layers are removed during the process. For others, e.g., compound casting, powder forming and sintering, cold roll bonding or adhesive joining, and deoxidation takes place prior to the process. Typically, a form of mechanical deoxidation is used like grinding or blasting in oxygen-free atmosphere. For some processes, thermal deoxidation is suitable depending on the material used. Chemical deoxidation is rarely reported. A tangible example for deoxidation during a process is laser beam brazing of aluminum alloys, where a pulsed laser beam with 45 ns pulse duration is employed for deoxidation.[46] At pulse energies of 60 μJ no deoxidation effect is observed. At 180 μJ, the existing oxide layer is reduced and the subsequent laser beam brazing process is facilitated (see Section 3.2 for further information). An emerging technique for deoxidation in the context of oxygen-free production is the application of DBDs as described a few sections earlier.

For future use, the method of deoxidation needs to be chosen depending on production process, material, necessary degree of reduction, and desired surface properties. Capital expenditure, energy consumption, complexity of machinery, and operating expenses should be considered.

2.4. Oxygen-Free Transport of Samples and Workpieces

Up to now, research in the field of oxygen-free production has been limited to a few selected and isolated production

**ADVANCED
SCIENCE NEWS**

www.advancedsciencenews.com

**ADVANCED
ENGINEERING
MATERIALS**

www.aem-journal.com

techniques. However, the positive results obtained so far suggest that in the future research in the field of oxygen-free production will be extended to many other production techniques and, especially, to production chains. If the production of a workpiece involves several processing steps and if the various production techniques required to manufacture the workpiece are located in separate process chambers, oxygen-free transport of workpieces may become necessary.

Similar considerations apply when the surfaces and interfaces of specimens manufactured in oxygen-free atmospheres need to be analyzed. Since the field of oxygen-free production has been largely unexplored so far, only little is known about the processes occurring at the surfaces and interfaces. Therefore, surface and interface analytical investigations play an important role in the research of oxygen-free production. If reoxidation of the surfaces prior to surface analysis needs to be prevented, oxygen-free transport from the process chambers to the analyzer must be ensured.

The easiest and most efficient way to transfer workpieces between separate process chambers is to use silane-doped argon atmospheres as well. The workpieces are stored within the silane-doped argon atmosphere of the process chamber in metal transport containers and sealed using either rubber or metal gaskets. To ensure oxygen-free conditions during transport, two factors are of essential importance: 1) the oxygen emission rate of the materials used and 2) the leakage rate of the sealing. In general, the emission rate depends only on temperature while the leakage rate furthermore increases with increasing pressure difference. Therefore, materials and techniques applied in vacuum technology must meet the highest requirements in terms of emission and leakage rate and are therefore the best choice for oxygen-free transport.

In vacuum technology, stainless steel (304, 316L) as well as aluminum are the most commonly used metal materials. They offer low outgassing and can be easily cleaned, for example, by heating in vacuum at elevated temperatures (150–250 °C). As sealings metal gaskets made of copper as well as rubber-elastic gaskets are common. Copper gaskets provide the best sealing effect. They are used in vacuum technology for ultrahigh vacuum conditions ($<10^{-10}$ mbar).

In the CRC, transport containers made of stainless steel are used. The containers are sealed by Viton seals and KF clamps. A sketch of such a transport container is depicted in **Figure 4**.

In order to evaluate the reliability of the transport containers, extensive experiments using titanium as test samples were carried out.[47] Titanium was used due to its high reactivity toward molecular oxygen. Exposing freshly deoxidized titanium surfaces

to argon atmosphere for 10 min resulted in an oxide layer of 2.3 nm. Conversely, 24 h exposure to silane-doped argon in a transport container including the lock processes resulted in an oxide layer thickness of 1.44 nm. The reoxidation in this case can be most probably attributed to residual water in the transport container.

### 2.5. Specialized Devices for Oxygen-Free Production

Research regarding production processes in oxygen-free environments is a young and evolving field. While working under oxygen-free conditions has numerous advantages, suitable equipment for each production process needs to be developed. For most of the ongoing research gastight glove boxes, mostly filled with silane doped argon, are employed. For some production processes devices for oxygen-free production have already been introduced, e.g., for resistance heating and simultaneous coating of metal sheets in oxygen-free conditions,[48,49] a plastic sheathing with gas inlet for the active area of milling and turning machines,[50] or a lab scale machine for oxygen-free LPBF, including the build chamber, powder management system, and gas circulation unit.[51]

3. Oxygen-Free Production Processes

In the following sections, results of published studies on oxygen-free production processes are described and discussed. Most of the results were generated within the framework of the CRC 1368.

3.1. Thermal Spraying

In thermal spraying processes, molten or heated particles are sprayed with high velocity onto a substrate. The processes are capable of generating thick coatings (>0.1 mm) with high deposition rates compared to other coating processes like physical or chemical vapor deposition. The resulting coatings are generally applied to enhance a certain surface property like corrosion or wear resistance. For these applications, strong adhesion of the coating to the substrate and strong cohesion in the coating are crucial. Porosity in the interface and between the coating that can be controlled by a careful adjustment of particle velocity, size, and temperature.[52] However, adhesion and cohesion strength are dominated by oxide layers. Conventionally, substrate surface preparation and the spraying process are carried out in air
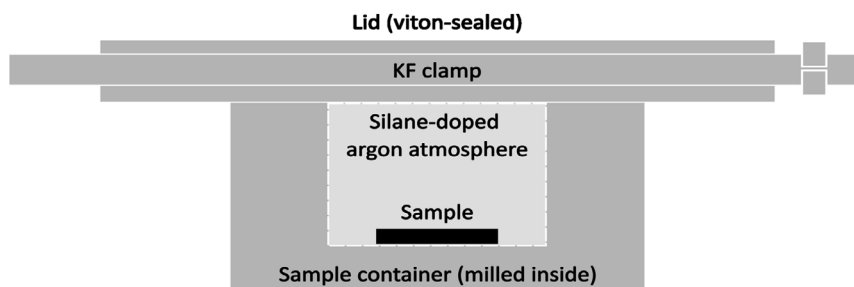
Figure 4. Transport container used to transport samples under oxygen-free conditions between separate process chambers.

ADVANCED
SCIENCE NEWS

www.advancedsciencenews.com

ADVANCED
ENGINEERING
**MATERIALS**

www.aem-journal.com

atmosphere resulting in interfacial and interlamellar oxide layers and impaired wetting behavior. These systematic defects limit the adhesion strength and the functional properties of the coatings. Established solutions to hinder oxide formation either limit the range of coating material (cold gas spraying) or still produce significant oxide layers due to comparatively high residual oxygen levels in rough vacuum or inert gas despite having a need for a more complex process technology (e.g., vacuum plasma spraying, vacuum induction plasma spraying).

Rodriguez Diaz et al. employed an oxygen-free atmosphere (silane in nitrogen, resulting in an oxygen content of 10^{-26} vol%) on a two-wire arc spraying (TWAS) process. Specifically, a coating chamber was designed to exclude the coating area from the surrounding air environment. The chamber was flooded with either air, nitrogen, or a nitrogen–silane mixture. As atomizer gas, these three alternatives were also investigated.[53] Additionally, a corundum blasting system was integrated into the chamber to enable a substrate surface preparation in the different atmospheres prior to the coating process.[54] Commercially pure copper (>99.8 wt% Cu) was sprayed on steel discs (steel grade S235JR, 1.0038). An overview showing the coating morphology obtained with spraying processes carried out in air (with air as atomizer gas) and in oxygen-free atmosphere (with silane in nitrogen as atomizer gas) is depicted in **Figure 5**. The cross section of the coating applied in oxygen-free atmosphere is free of inner oxide layers and features a porosity that is reduced to one-third compared to the reference produced in air .[20] Since the coatings were produced with the same process parameters and air and nitrogen feature similar properties in terms of arc duration and thermal conductivities, these significant improvements can be attributed primarily to the oxygen-free atmosphere.
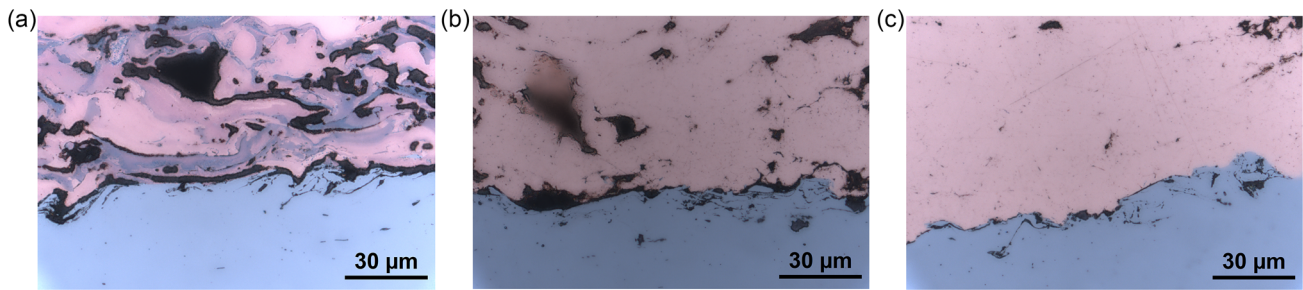
It is already obvious from Figure 5 that the gaps between the substrate and the coating were also significantly reduced. This can be further improved by carrying out the corundum blasting process in the oxygen-free atmosphere. **Figure 6** shows the effect of a blasting process carried out in different atmospheres. When the blasting process is also carried out in oxygen-free atmosphere, the wetting behavior of the impacting particles is significantly improved in the subsequent spraying process. Hence, additional bonding mechanisms between the substrate and the coating can be activated compared to conventional TWAS.[55]

This is also shown in the adhesive tensile strength (ATS) tests carried out by Rodriguez Diaz et al. The tests were carried out in accordance with the standard DIN EN ISO 14 916 (sample type B) using Ultrabond 100 as the adhesive. **Figure 7** depicts the results of those tests. When blasting and coating were carried out in air, cohesive coating failure leads to an ATS of 25.1 ± 0.4 MPa (Figure 7 I). When the coating process was transferred to the oxygen-free atmosphere, an increase in ATS by 39% (Figure 7 II) was observed, and the failure mechanism changed to pure adhesive coating failure. The measured ATS for that process combination is in good accordance to coatings produced in nitrogen atmosphere.[56] Transferring the blasting process to the oxygen-free atmosphere leads to an additional significant increase in ATS to values between 46.8 ± 4.4 MPa and 63.9 ± 3.0 MPa (Figure 7 III to V). Compared to the conventional process in air, this is an increase between 85% and 150%. High variance between the sample sets III to V indicates that small differences in the blasting and coating have a substantial impact. However, the failure mode of the sample set V was solely the failure of the employed Ultrabond 100 adhesive. Hence, even
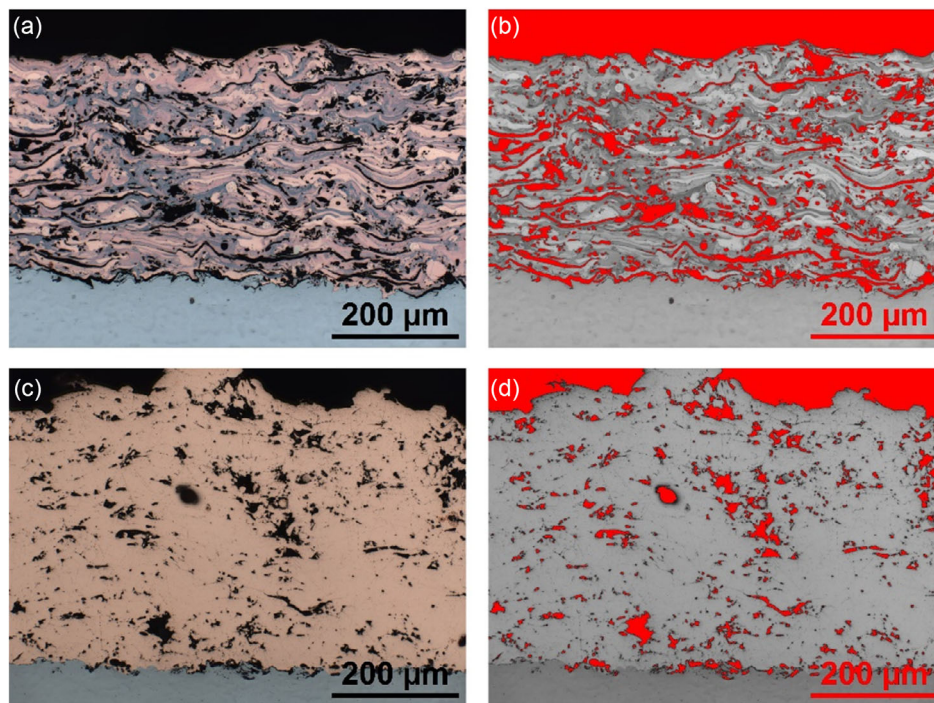

Figure 5. Micrographs of cross sections of thermal sprayed copper coatings on steel substrate: a) sprayed in air, b) corresponding porosity analysis, c) sprayed in oxygen-free atmosphere, d) corresponding porosity analysis. Reproduced with permission.[54] Copyright 2022, The Authors, published by MDPI.

**ADVANCED
SCIENCE NEWS**

www.advancedsciencenews.com

**ADVANCED
ENGINEERING
MATERIALS**

www.aem-journal.com

Figure 6. Difference in interfacial gaps between copper coatings and steel substrate: a) blasted and sprayed in air, b) blasted in air, sprayed in oxygen-free atmosphere, c) blasted and sprayed in oxygen-free atmosphere. Reproduced with permission.[55] Copyright 2022, The Authors, published by MDPI.
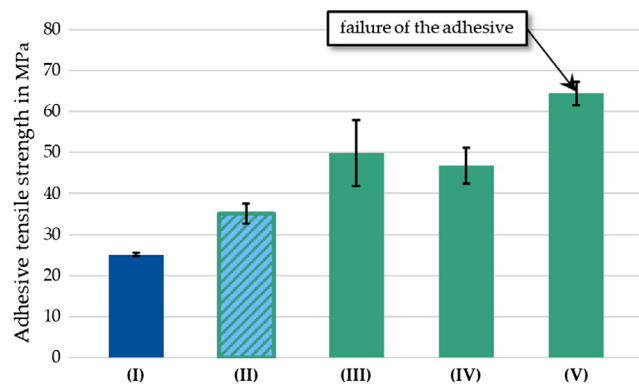
Figure 7. Adhesive tensile strengths (ATS) of copper TWAS coatings on steel substrates determined according to DIN EN ISO 14 916 standard. I: blasted and coated in air, II: blasted in air, coated in oxygen-free atmosphere, III–V: blasted and coated in oxygen-free atmosphere. Reproduced with permission.[54] Copyright 2022, The Authors, published by MDPI.

higher ATS might be possible for the material system when employing the oxygen-free atmosphere. This shows the potential to revolutionize the field of thermal spray coating by employing the concept of oxygen-free production.

3.2. Laser Beam Brazing

Laser beam brazing is a method widely used for joining metal parts during the production of the outer shells of car bodies. Presently, the industrial use of laser beam brazing is typically restricted to joining galvanized steel.[57,58] Brazing of aluminum alloys is more challenging and usually requires the use of corrosive fluxes, as the native oxide layer present on the aluminum alloys prevents wetting and diffusion between the filler material and the sheet metal during the joining process. While it has been shown that laser pulses in the nanosecond regime can break up the oxide layer of aluminum alloys,[59] the problem of re-oxidation remained unaddressed.
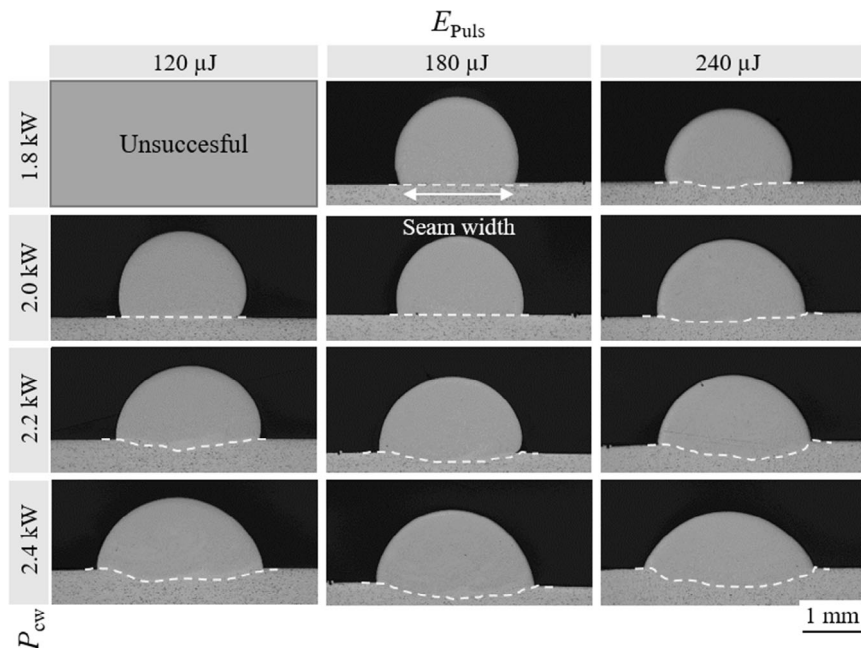
Aman et al. illustrate that laser beam brazing of aluminum alloys in an oxygen-free atmosphere efficiently prevents reoxidation, while at the same time facilitating the removal of the oxide layer, thereby making the use of flux obsolete.[60] In their work,

Aman et al. used a setup of two laser beam sources, a pulsed (pw) laser beam source for removal of the oxide layer with pulses in the nanosecond regime and a continuous wave (cw) laser beam source for the brazing process. The process was performed inside a glove box, which was filled with silane-doped argon providing an oxygen-free atmosphere. As substrate the aluminum alloy AlMgSi1 (EN AW-6082) was used, and AlSi12 (EN AB-44 100) was employed as the filler wire.

The first experiments with a cw spot diameter of 5 mm and superimposed cw and pw laser beams showed promising changes in wetting angle for oxygen-free conditions, cf. **Figure 8**. At a laser beam power of $p_{cw} = 2.3\,kW$ and a pulse energy of $E_p = 120\,\mu J$, the wetting angle of the seam was over 70° for argon atmosphere, around 50° for flux (FL20) supported brazing (without pw oxide removal) and approx. 40° for seams brazed in silane-doped argon.[60] While flux brazed reference seams exhibited a regular shape and their cross sections showed no signs of melting of the substrate, this was not the case for samples brazed in argon and silane-doped argon. This difference is apparent in cross-sectional views where a slight melting of the base material is visible for argon and a much more pronounced melting occurs in argon silane. This effect is attributed to higher energy absorption of the silicon dioxide particles that are present on the sheet surface due to the reaction of the silane with the residual oxygen present in the atmosphere. Brazing aims at inducing only minor changes to the base material during the process. The challenge for Aman et al. was to find parameters where wetting and diffusion occur in oxygen-free atmosphere paired with a negligible extent of base material melting.

Adjusting the spot diameter of the cw source to 2.9 mm and deoxidizing with the pw beam prior to brazing with the cw beam instead of using superimposed beams led to significantly less melting of the base material in silane-doped argon atmosphere but higher wetting angles.[46] Seams produced at various laser beam powers p_{cw} and pulse energies E_p of 120 μJ or 180 μJ feature sufficient wetting angles without critical melting of the base material and exhibit a metallurgical bond as shown in Figure 8. Experiments in argon at similar parameters did not produce a seam even at $p_{cw} = 2.4\,kW$ and $E_p = 240\,\mu J$. A visual comparison of seams brazed in argon and silane-doped argon atmosphere, respectively, is given in **Figure 9**.

Aman et al. tested this approach for aluminum alloys with high magnesium content, e.g., AlMg3 (EN AW-5754), which

**ADVANCED
SCIENCE NEWS**

www.advancedsciencenews.com

**ADVANCED
ENGINEERING
MATERIALS**

www.aem-journal.com

Figure 8. Cross-sections of bead on plate seams brazed under silane-doped atmosphere on AlMgSi1 with a wire feed of 2.0 m min^{-1}. Reproduced with permission[46] Copyright 2022, Elsevier.
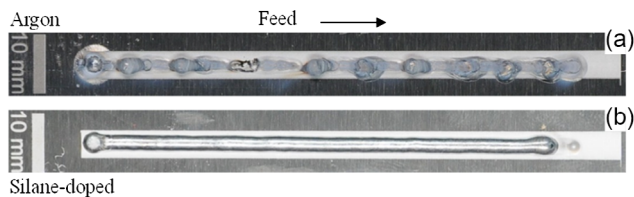
Figure 9. a) Comparison of bead on plate seams brazed under pure argon and b) silane-doped argon atmosphere with $p_{cw} = 2.4$ kW and $E_{Puls} = 240$ µJ on AlMgSi1. Reproduced with permission[46] Copyright 2022, Elsevier.

are only brazeable with corrosive fluxes.[46] Melting of the base material already occurred at low laser beam powers of around 1.4 kW, therefore the challenge to increase the seam quality while reducing melting remains for those alloys. On the microscopic scale, wetting angles of around 30° were achieved for AlMgSi1, here the challenge is to achieve those angles on the macroscopic scale as well.[60] Although those issues still need to be addressed in future studies, laser beam brazing in oxygen-free atmosphere is a promising route for joining aluminum alloys without fluxes.

3.3. Compound Casting

Compound casting of liquid aluminum onto a solid copper part offers great potential to generate bonds with high thermal conductivity between these two materials. Typical applications of this material combination can be found in cooling solutions for electric components when cost and specific weight reduction are of interest as copper features the thermal conductivity and

aluminum low density and low cost.[61] However, typically these metals are either joined mechanically (often with the use of thermal paste to bridge the inevitable gap) or by soldering processes that are oftentimes unable to join the complete interface. Composite casting can overcome the limitations resulting from the above processes in terms of the thermal conductivity of the bonding. Oxide layers of the involved metals generally hinder the diffusion process for the formation of a metallurgical bond in compound casting, which is why direct compound casting without further measures is usually not successful with the material combination aluminum–copper.[62]

Fromm et al. investigated the effect of transferring the compound casting process of aluminum on copper into an oxygen-free atmosphere. For this, a gravity-casting set-up was placed inside a glove box filled with the oxygen-free atmosphere described in chapter 2.1. The aluminum was molten inside a graphite crucible by induction heating, and the mold with the copper inlay could be preheated by carefully placed resistance coil heating elements.[61] The copper surfaces were cleared of their natural oxide layer by grinding with 500 and then 1200 grit abrasive papers. Compound castings were carried out with a variety of combinations of crucible and mold temperature. The temperature of the copper inlays can be approximated to be roughly equal to the mold temperature. The compounds were then analyzed regarding the thickness and the thermal conductivity of the overall compound zone. Additional analysis of the phases present in the compound zone revealed a region with a eutectic structure of α-Al with Al$_2$Cu and layers of Al$_2$Cu, AlCu, and Al$_4$Cu$_9$ intermetallic phases (in that order from Al to Cu).

In **Figure 10**, the total measured thickness of the compound zones depending on crucible and mold temperature is depicted. With mold temperatures of 300 °C, it was only possible to
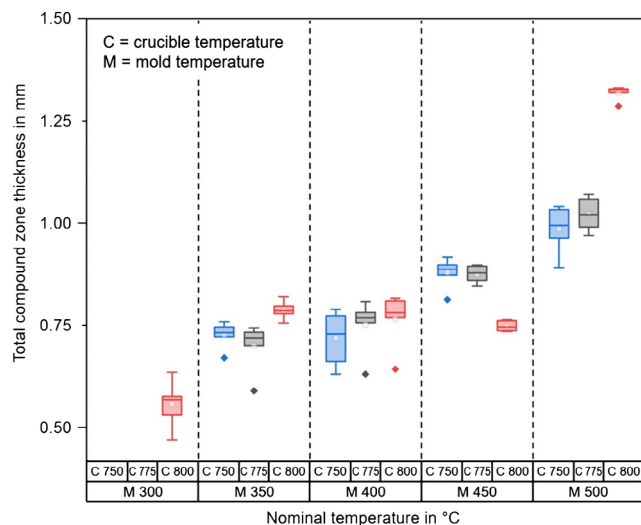
Figure 10. Total compound zone thicknesses of specimens cast with different process temperatures. Reproduced with permission.[62] Copyright 2022, The Authors, published by Springer.

Figure 11. Comparison of the data obtained by Fromm et al.[62] (orange and blue) in comparison to literature results from ref. [79,80]. Reproduced with permission.[62] Copyright 2022, The Authors, published by Springer.

generate a full bond with the highest tested crucible temperature. Obviously, the mold temperature had a much stronger influence on the compound zone thickness than the crucible temperature which was attributed to the high thermal conductivity of copper.[62] Generally, it is possible to control the compound zone thickness over a wide range by carefully adjusting the process temperatures.

The influence of the overall compound zone thickness on thermal conductivity showed—on one hand—that smaller compound zones generally tend to feature a higher thermal conductivity. However, different casting parameters that resulted in a similar compound zone thickness could also feature quite different thermal conductivities, probably due to the thermal conductivities of the phases involved. Hence, special attention has to be paid to the composition of the compound zone and the thickness of the individual phases.

Figure 11 depicts a comparison to the thermal conductivities measured in earlier studies for processes currently employed in the industry. Compound casting leads to much higher values than mechanical connections with thermal paste and can reach values of state of the art processes like soldering or compound casting with intermediate layers.[62] Compared to soldering, compound casting is capable to join much larger surfaces. Hence, new products with high interfacial thermal conductivity might be possible. The fact that no additional intermediate layer and consequently no additional coating process is needed when compound casting is carried out in an oxygen-free environment offers potential for higher productivity and reduced production costs.

3.4. Friction and Wear Behavior in Oxygen-Free Atmospheres

During production processes involving wear, titanium alloys frequently exhibit rapid surface reoxidation in normal atmosphere.
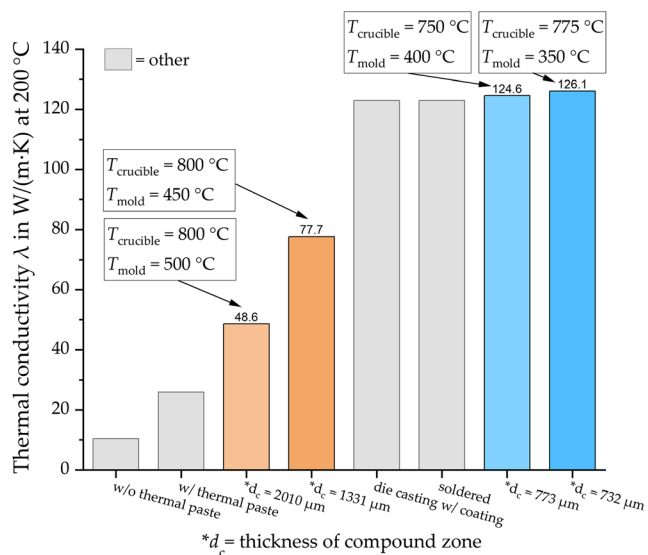
This causes high wear in tribological systems. Raumel et al. hypothesize the occurrence of different wear mechanisms in oxygen-free atmosphere.[63] They assume that without an oxide layer and no residual oxygen in the process atmosphere, the differences in the chemical reactions, adhesion, diffusion, hardness and lubricating effects change the wear behavior depending on the composition of the alloy. To verify their claim, Raumel et al. use an encapsulated universal high-temperature tribometer with gas inlets to set different atmospheres and adjust the processing temperature.[63] The parameters of their ball-on-disc experiments with Ti–6Al–4V and copper discs are given in **Table 1**.

3.4.1. Wear Behavior of Ti–6Al–4V in Oxygen-Free Atmospheres

Ball-on-disc friction tests were performed in air, argon, and silane-doped argon (oxygen-free) with Ti–6Al–4V discs and

Table 1. Parameters for ball-on-disc experiments on Ti–6Al–4V and copper discs. The parameters are extracted from ref. [63] for Ti–6Al–4V and[64] for copper.

Parameter	Ti–6Al–4V	Copper
Ball material	Tungsten carbide	Copper
Ball diameter	2 mm	2 mm
Normal force	7 N	2 N
Surface pressure	2.4 GPa	1.2 GPa
Reference contact area	0.02 mm^2	0.0084 mm^2
Sliding distance	160 mm	160 mm
Sliding speed	62.8 mm min	62.8 mm min
Temperature regime	RT–1000 °C	RT–800 °C

**ADVANCED
SCIENCE NEWS**

www.advancedsciencenews.com

**ADVANCED
ENGINEERING
MATERIALS**

www.aem-journal.com

tungsten carbide balls as friction partners.[63] **Figure 12** shows Ti–6Al–4V discs after friction tests in different atmospheres at 1000 °C. The discs show different visual impressions depending on the atmosphere. Raumel et al. report a 10 μm-thick oxide layer consisting mainly of TiO_2 in rutile structure with an Al_2O_3-rich top layer after ball-on-disc tests in air at 1000 °C.[63] In argon atmosphere, the oxide layer thickness in similar tests amounts to ≈ 2 μm. While consisting mainly of TiO_2 in rutile structure with an Al_2O_3 rich top layer, small amounts of understoichiometric Ti_3O are present. There is no distinct oxide layer, but rather a thin layer containing silicon detectable by SEM after experiments in silane-doped argon atmosphere. X-ray diffraction (XRD) shows a distortion of the titanium lattice, which, according to Raumel et al., is not caused by titanium hydrides. Silicon is assumed to occupy interstitial defects thereby causing the lattice distortion. For further information on the EDX or XRD analysis, the reader is referred to ref. [63].

Roughness in the friction marks of the discs after ball-on-disc testing and on the disc surfaces in general is the lowest for samples tested in silane-doped argon atmosphere. With increasing temperature, the hardness of samples tested in oxygen-free atmosphere increased from 5.6 to 9.6 GPa, while it decreased from 5.6 to 1.7 GPa in air.

In air, the friction coefficient rises with increasing temperature up to 0.6 at 1000 °C, while remaining nearly constant over that temperature range in argon atmosphere.[63] The friction coefficient in oxygen-free atmosphere exhibits a more complex behavior, rising sharply from room temperature up to 200 °C, decreasing up to 600 °C, and increasing again up to 0.5 at 1000 °C. According to Raumel et al., the increase up to 200 °C is caused by a diminishing oxide layer due to mechanical abrasion and suppressed reoxidation in oxygen-free conditions. The resulting adhesion causes the friction coefficient to rise. At higher temperatures, the friction coefficient drops due to the formation of a friction reducing layer of increasing hardness. Above 600 °C, this effect is superimposed by the increasing chemical activity at high temperatures causing the friction coefficient to rise again. The wear volume increases with rising temperature in all atmospheres, but the magnitude depends drastically on the particular atmosphere. While increasing by over 550% of its room temperature value in air at 1000 °C, the increase of wear volume in silane-doped argon amounts to about 20% at 1000 °C.[63]

3.4.2. Wear Behavior of Cu in Oxygen-Free Atmospheres

Ball-on-disc tests with copper were performed in different atmospheres ranging from room temperature up to 800 °C.[64] As in the case of the titanium alloy described earlier, the roughness of the sample surface is significantly lower after the tests in silane-doped argon atmosphere compared to air. The apparent Young's modulus as determined by nanoindentation increases by about 56% with temperature rising from room temperature to 800 °C in silane-doped argon atmosphere, while decreasing 66% and 69% in argon and air, respectively. The hardness increases sharply starting at 600 °C in silane-doped argon, while decreasing in air and showing only a minor increase in argon atmosphere.

As in the case of Ti–6Al–4V, the wear volume in ball-on-disc tests on copper increases in air, argon, and silane-doped argon atmospheres with rising temperature.[64] Raumel et al. report a room temperature value of 37 $μm^3$ for all atmospheres, at 800 °C this value increases by about 300% in air, more than 100% in argon and 50% in silane-doped argon. As with the wear of Ti–6Al–4V, the comparably small increase of wear volume under oxygen-free conditions is attributed to suppressed tribochemical wear. Friction coefficients are higher for silane-doped argon compared to the other atmospheres, with the most pronounced differences in the temperature range from 200 to 600 °C.

On the surface of the sample tested in air (30 min, 800 °C) a 10 μm-thick oxide layer consisting of mainly of Cu_2O and small amounts of CuO had formed,[64] while samples tested in argon exhibited an oxide layer with a thickness of 2 μm consisting mainly of Cu_2O. Samples tested in silane-doped argon did not exhibit an oxide layer detectable with EDX. Two different zones form as visible in **Figure 13**. XRD analysis reveals the formation of η-Cu_3Si in addition to the copper cubic matrix at point MP1. The precipitations at MP2 consist mainly of η-Cu_3Si with smaller amounts of γ-Cu_5Si and ε-$Cu_{15}Si_4$ as well as traces of SiO_2 in form of a thin film caused by sample transfer in air.

Figure 12. Ti–6Al–4V discs after ball-on-disc tests at 1000 °C in different atmospheres—from left to right—silane-doped argon, air, and argon (Photograph provided by Selina Raumel).
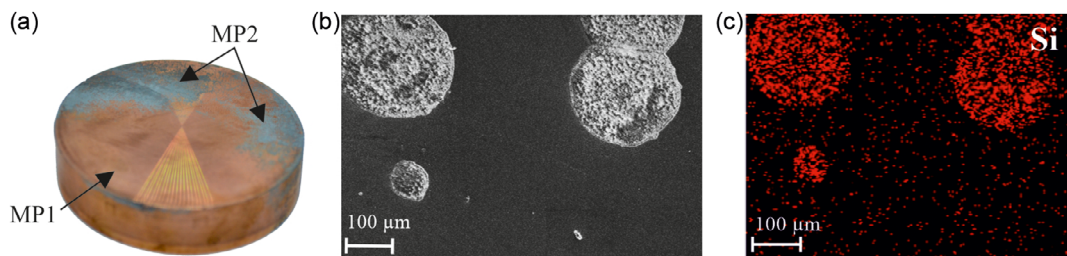
Figure 13. Copper sample treated under argon-silane atmosphere showing two different surface areas: MP1—metallic pure copper and a) MP2—pitting zone; b) SEM and c) EDS analysis of the Si deposits on the Cu sample. Reproduced with permission.[64] Copyright 2023, The Authors, published by Springer.

The suppression of reoxidation and the absence of brittle oxide layers cause a significant reduction of tribochemical wear for Ti–6Al–4V and Cu, resulting in a significant reduction of wear volume in oxygen-free atmosphere compared to tests conducted in air.[63,64] These results indicate a possible expansion of the application range of Ti–6Al–4V beyond currently possible operating temperatures, if wear is the dominating damage mechanism.[63] For Cu no significant increase in contact resistance even at 800 °C was detected in silane-doped argon atmosphere, this may improve applicability in electronics.[64] Copper silicides that emerge during processing in silane-doped argon may protect Cu from further oxidation and corrosion and offer advantages for the production of integrated circuits.

### 3.5. Cutting of Titanium Alloys in Oxygen-Free Atmosphere

Cutting of titanium alloys is correlated with high temperatures at the interface of tool and workpiece.[65,66] This can foster a fast build-up of adhesion on tools and consequently leads to high adhesive wear and increased susceptibility to diffusion and tribochemical reactions. Maier et al. state that tribooxidation is causing excessive wear when dry milling titanium alloys.[50] They suggest the elimination or reduction of tribooxidation in oxygen-free atmospheres formed, e.g., by silane-doped argon. Conventional protective gas atmospheres are not sufficient due to traces of oxygen especially with the high oxygen affinity of titanium alloys.

During dry milling of Ti–6Al–4V in oxygen-free atmosphere Maier et al. observe far less adhesion of the titanium alloy forming a built-up edge on flank and rake faces compared with dry milling in air (cf. **Figure 14**).[50] Feed forces were about 70% lower in silane-doped argon atmosphere compared with air. The authors explain this effect by the change in edge micro geometry due to profound adhesion in air. A rounding of the edge generally leads to higher cutting and feed forces with the latter reacting more sensitively to rounding.[67]

Furthermore differences in chip formation occur, the chip curl radius after milling in silane-doped argon is increased by 16% with respect to milling in air.[50] The curl radius depends on thermal properties of the workpiece material and the friction behavior between workpiece and tool.[68,69] The chips forming in oxygen-free atmosphere are longer. More pronounced chip segmentation is observed in air.[50] Increased chip segmentation is a sign of higher temperature in the deformation zone of the chip, thus indicating lower effect zone temperature when dry milling in silane-doped argon.

Denkena et al. investigated the tribochemical wear resistance of TiN, TiAlN, and CrAlN coated carbide tools in different atmospheres during turning of Ti–6Al–4V. The tool life of TiN- and TiAlN-coated carbide tools was much shorter with respect to uncoated tools due to tribochemical wear regardless of process atmosphere.[70]

CrAlN on the other hand shows high wear resistance and is a promising coating for high-temperature cutting applications.[71]
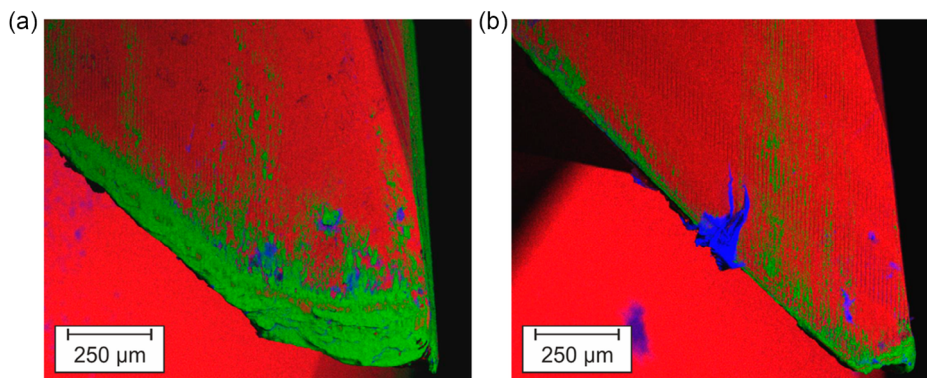
Figure 14. EDX elemental mappings showing the distribution of titanium on the tool in green after milling in a) laboratory air and b) an XHV-adequate environment (red: tungsten; blue: carbon). Reproduced with permission.[50] Copyright 2020, The Authors, published by MDPI.

However, oxidation of the coating at high temperatures poses a problem for these applications. Removing oxygen from the process atmosphere resulted in increased tool life by 60%.[70] The tool life in argon atmosphere is between that of air and oxygen-free atmosphere. Denkena et al. attribute the increase in tool life to decreasing tribochemical wear. Notch wear is observed for turning in air and mostly flank wear in argon and silane-doped argon. Uncoated tungsten carbide tools exhibit an increase in tool life with decreasing oxygen content of the processing atmosphere, albeit the effect is not as pronounced as in the case of CrAlN.[70] In absolute values, uncoated tungsten carbide shows slightly longer tool life compared to CrAlN-coated tools.

Schaper et al. compare turning of Ti–6Al–4V with different tool materials and vary the oxygen content of the processing atmosphere. A slight effect of increasing tool life with decreasing oxygen content is observed for tungsten carbide.[72] The authors assume that the reason for this is suppressed scale formation in silane-doped argon. Other cutting materials, e.g., polycrystalline diamond (PCD) or cubic boron nitride (cBN) behave differently in this context ranging from no effect at all to decreased tool life. While binder materials that contain titanium and a change in friction and wear behavior are assumed to have an influence, the causes are still subject of ongoing research.

Contrary to the study on dry milling titanium alloys in oxygen-free atmosphere,[50] Schaper et al. report increased adhesion during turning in oxygen-free atmosphere.[72] While the cause remains to be determined, lower temperature during milling, lower cutting speed during milling, or the use of cBN in the turning process might be the reason.

Prasanthan et al. analyzed chip formation and surface properties of Ti–6Al–4V components machined by longitudinal turning at a cutting speed of $60\,\mathrm{m\,min^{-1}}$.[73] They found lengthened strip chips in air and curled chips in oxygen-free environment. The approximately 15% smaller chip thickness in air hints toward a change in chip formation mechanism. The core roughness of machined specimens determined from Abbott curves is reduced by around 25% and residual stress fluctuations in circumferential direction of a longitudinally turned specimen seem to be reduced in oxygen-free atmosphere compared to air.[73]

In general, cutting in oxygen-free atmosphere has a strong influence on process, component behavior, and component surface properties of Ti–6Al–4V.

3.6. Resistance Heating with Simultaneous Coating for Hot-Stamping Applications

Hot stamping is a forming technology typically applied in the production of automotive body components requiring high tensile strength. Sheets of manganese boron steel (typically 22MnB5) are heated up above austenite finish temperature in a gas-powered roller hearth furnace and are subsequently formed and quenched in a cooled forming tool to induce a martensitic phase transformation. The martensitic microstructure that emerges during cooling is responsible for high tensile strength. However, steel surfaces exposed to oxygen and elevated temperatures exhibit scale formation. During conventional hot stamping, this is prevented by precoating the sheet metals with AlSi coatings.

Significant problems of hot stamping processes are high energy needs and long processing times during heating of the sheets in the roller hearth furnaces. A possible solution could be rapid resistance heating.[49] However, for resistance heating, conventional AlSi coatings cannot be employed as long holding times at elevated temperatures are required for the formation of the necessary intermetallic Fe–Al phases. Thus, without an appropriate coating, scale formation occurs during resistance heating (primary scale formation) and upon workpiece transport to the forming tool (secondary scale formation).

Behrens et al. developed a new approach to hot stamping of 22MnB5 where they combined resistance heating without AlSi protection in oxygen-free atmospheres with simultaneous coating .[14,41] The oxygen-free atmosphere prevents primary scale formation during heating. The application of suitable coatings also prevents the formation of secondary scale. 22MnB5 steel sheets were simultaneously heated and coated in a custom-built chamber under silane-doped nitrogen atmosphere.[49,74] The sheets were precoated with Ni700 by applying an organically bound powder before resistance heating.

Figure 15 shows a component after resistance heating and coating in oxygen-free atmosphere as well as subsequent hot stamping. The middle section of the component is coated with Ni700 and does not exhibit scale formation. On both sides of the coated area, regions with minor secondary scale formation are visible. These areas were not precoated with Ni700 but were included in the sealed oxygen-free chamber during heating. The outermost parts of the component were exposed to ambient atmosphere during heating, and thus exhibit the most pronounced scale formation.

Behrens et al. found defect-free bonding of the Ni700 coating to the base material over large surface areas at process temperatures between 900 and 980 °C, while no scale formation occurred.[49] Subsequent hot stamping did smooth out the surface of the coating, and no cracks reaching the base material
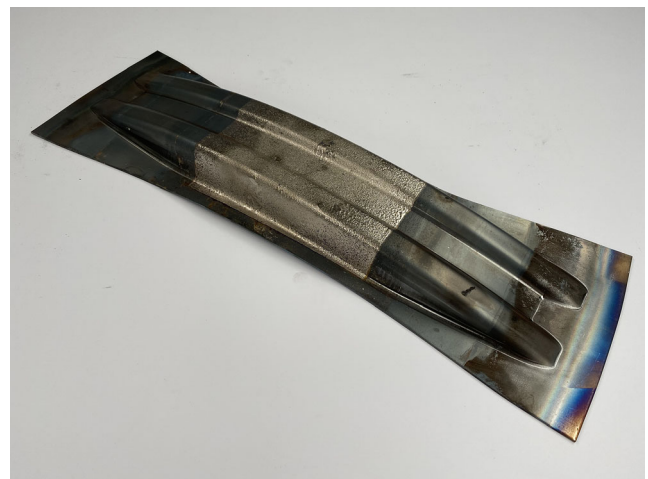
Figure 15. Workpiece after resistance heating, simultaneous coating in oxygen-free atmosphere and subsequent hot stamping (photograph provided by Lorenz Albracht).

occurred at low degrees of forming.[49] However, at high forming degrees, cracks were observed in the base material.[74]

While future challenges, e.g., the development of crack-free coatings of homogeneous thickness remains to be addressed, the works show that resistance heating in oxygen-free atmosphere is a promising approach to prevent scale formation. In addition, this approach can enable significant energy savings in hot-stamping processes.

3.7. Other Production Processes in Oxygen-Free Atmosphere

Several other production processes were performed under oxygen-free conditions in the past years as well, which demonstrated that oxygen-free environments can be employed to improve a wide range of production processes. However, the full potential could not be exploited in all cases yet. In addition, there are other production processes, which may benefit from oxygen-free conditions but have not yet been under investigation, some hints are given in Section 4.

3.7.1. Inert Gas Brazing in Silane-Doped Atmosphere

Several researchers describe adding monosilane to the atmospheres used in high-temperature brazing processes in order to improve brazed joint quality.[11,12,75] Processes can be separated into furnace processes in silane-doped atmosphere[12] or silane addition to a shielding gas flow.[11]

Reisgen et al. correlated monosilane addition during TIG arc brazing with shielding gas to properties of the brazed joints. They observed a decrease of the wetting angle of CuAl7 on S235JR to 36° with increasing silane addition to the shielding gas flow up to $0.6\,L\,min^{-1}$ of 1% silane in argon.[11] Holländer et al. describe the successful joining of stainless steel with a Cu braze in silane-doped argon, a process which usually requires a hydrogen atmosphere in the furnace as well as joining titanium and WC/Co hard metal with $Ag_{72}Cu_{28}$ braze in silane-doped argon, normally requiring high-vacuum conditions.[12]

3.7.2. Roll Bonding

Roll bonding is a process for producing material composites based on an adhesive bond between two or more joining partners. However, the possible material combinations are so far severely limited. Even minor impurities and thin oxide layers in the contact area of the joining partners reduce the surface energy and consequently make it difficult to form a uniform and stable joint zone. By transferring the surface preparation (deoxidation) and roll bonding process into an oxygen-free atmosphere, the formation of new passivating oxide layers is inhibited and bonding during rolling is facilitated. First results for aluminum-copper bondings show a decrease in the minimum degree of deformation needed for the formation of a solid bond by up to 35%.[76]

3.7.3. Additive Manufacturing by Laser Powder Bed Fusion

During LPBF, the residual oxygen content in the processing atmosphere leads to the fast formation of oxide layers and problems like "balling" and embrittlement due to oxygen incorporation, especially for materials with high oxygen affinity. This decreases the quality of the produced components.

Emminghaus et al. observed changes in density, porosity, and microstructure of LPBF-built Ti–6Al–4V components as well as changes in the LPBF process itself, such as different wetting behavior and spatter formation when processing in oxygen-free atmosphere.[51] They developed a lab scale LPBF system where all process steps can be carried out in oxygen-free atmosphere. Results of complete LPBF-manufacturing in oxygen-free atmosphere are not yet published. But the influence of silicon dioxide particles, which form during processing of powders in silane-doped argon on properties of LPBF-built Ti–6Al–4V components, was investigated. While no effects of SiO_2 particles on roughness, porosity or hardness of the produced components was detected, the flowability of the powders was improved.[77]

3.7.4. Grinding Tool Wear

Grinding of Ti–6Al–4V by bronze-bonded tools results in high tribooxidation. An oxygen-free atmosphere may therefore increase tool life. Unpublished results by Denkena, Bergmann, and Hansen show a substantial decrease of tool wear for cubic boron nitride (Cbn) grinding tools compared to grinding in air, thus increasing the tool life in oxygen-free atmosphere. In contrast, tool life of diamond tools did not differ significantly between grinding in air- or oxygen-free atmosphere.

3.7.5. Adhesive Bonding

Many adhesives need certain constituents of the process atmosphere like oxygen or water to initiate or facilitate the curing process. Changing the amounts of those constituents allows for control of the curing process. In adhesive application, pot lives that are either too short or too long are detrimental to process efficiency. Cyanoacrylate cures due to the residual water content in atmospheric air within seconds. Unpublished results by Gerland, Moritz and others show a comparison of cyanoacrylate adhesive joints of aluminum processed in air, argon, and silane-doped argon. Cyanoacrylate joints in argon atmosphere show slower curing and significantly lower tensile strength after 72 h compared with atmospheric air. Joints in silane-doped argon did cure slower, while their tensile strength was similar to those processed in atmospheric air.

4. Conclusions and Outlook

The previous sections substantiate the claim that oxygen-free conditions in production processes generate a huge variety of effects, many of them beneficial. The long-term aim is ultimately to achieve a cross-material and cross-process understanding of the possibilities and mechanisms of oxygen-free production.

Most of the presently published research is focused on the interaction zone (e.g., contact zone during joining, tool engagement during cutting) of the processes. Either the interaction zone is kept free of oxygen by means of providing an oxygen-free atmosphere or the space around the interaction zone is encapsulated and consist of an oxygen-free atmosphere. The present range of

**ADVANCED
SCIENCE NEWS**

www.advancedsciencenews.com

**ADVANCED
ENGINEERING
MATERIALS**

www.aem-journal.com

materials processed and/or deoxidized in oxygen-free atmosphere includes many pure metals and some hard to process alloys such as Ti–6Al–4V. The former facilitate the understanding of effects taking place in oxygen-free conditions, while the latter are expected to show radically different behavior under such conditions. Since new behavior is to be expected at the interaction zone in many production processes due to the absence of oxygen and deoxidized surfaces, a fundamental understanding of the processes and mechanisms involved in the contact of oxide layer-free (metal) surfaces must be established regarding advantageous effects as well as detrimental ones. For some of the described processes in Section 3, an understanding is already established, while other effects lack a fundamental explanation up to now. Suitable models need to be investigated in the future to fulfill the overarching aim of cross-material and cross-process insights.

As several of the researchers involved in oxygen-free production state in their publications, the range of materials considered should and will be expanded in future research. The knowledge gained from effects on pure metal surfaces will in many cases be transferred to alloys relevant in industrial use. Furthermore, an expansion to different classes of materials is conceivable, e.g., ceramic materials and plastics. Besides expanding the variety of materials, the effective area under consideration should be increased in the future to transfer the effects investigated in the interaction zone to entire processes. Implementing oxygen-free atmosphere for complete process chains is the long-term vision. If oxygen-free production processes are to become industrial practice, not only feasibility and technical implementation but also economic viability of the process chains needs to be addressed. So far only a fraction of possible production processes is under investigation for potential benefits due to oxygen-free production, this number may increase in the future. For example, while some coating techniques like thermal spraying already give astounding results in oxygen-free atmosphere, the effects of such an atmosphere on a host of other coating techniques are not explored yet.

Creating oxygen-free and oxide-free conditions requires a certain effort. Whether oxygen-free production will ever become reality is a legitimate question. Most probably oxygen-free conditions are not suitable for every production process, only certain production chains will benefit. Oxygen-free production can 1) enable processes that were impossible before or 2) result in processes that are better by orders of magnitude regarding cost or quality compared to their conventional counterparts. Processes exhibiting small improvements by working in oxygen-free atmosphere may be constrained by the necessary efforts to create the atmosphere. A good example for 1) is wire arc spraying of high-quality functional titanium layers, which was previously unfeasible and there is reason to assume similar breakthroughs in other areas.

The ongoing research on oxygen-free production opens up an interesting perspective, the use of oxygen-free atmospheres in other fields of research, not only for altering production processes. A good example is the field of electrochemistry, where a lot of deposition processes take place in oxygen and water sensitive electrolytes, e.g., certain ionic liquids. State of the art is the use of inert gases, which contain residual amounts of oxygen, whose influence on the deposition process as well as surface oxidation of the deposited film can be eliminated by using an oxygen-free atmosphere. Other possible areas include replacing UHV, analytical methods like atomic force microscopy in oxygen-free atmosphere, or the generation of oxygen-free materials in the first place.

Conflict of Interest

The authors declare no conflict of interest.

[1] A. J. Sedriks, Corrosion of Stainless Steels, **2001**.

[2] C. Strauß, R. Gustus, W. Maus-Friedrichs, S. Schöler, U. Holländer, K. Möhwald, *J. Mater. Process. Technol.* **2019**, *264*, 1.

[3] R. Hoffmann, *HTM J. Heat Treat. Mater.* **1984**, *39*, 99.

[4] J. E. King, *Mater. Sci. Technol.* **1990**, *6*, 19.

[5] W. S. Miller, L. Zhuang, J. Bottema, A. J. Wittebrood, P. De Smet, A. Haszler, A. Vieregge, *Mater. Sci. Eng. A* **2000**, *280*, 37.

[6] J. J. Stephens, *Brazing and Soldering: Proceedings of TheThird Inter. Brazing and Soldering Conf. April 24-26, 2006*, San Antonio, TX, **2006**.

[7] Q. Wu, J. Gong, G. Chen, L. Xu, *Opt. Laser Technol.* **2008**, *40*, 420.

[8] K. Weman, G. Lindén, *Mig Welding Guide*, Woodhead Publishing, Sawston **2006**.

[9] E. Roman, M. Sánchez-Avedillo, J. L. de Segovia, *Appl. Phys. A* **1984**, *35*, 35.

[10] S. Hofmann, *Auger- And X-Ray Photoelectron Spectroscopy In Materials Science: A User-Oriented Guide*, Springer, Heidelberg; New York **2013**.

[11] U. Reisgen, K. Willms, G. Buchholz, *Soldag. Insp.* **2015**, *20*, 315.

[12] U. Holländer, D. Wulff, A. Langohr, K. Möhwald, H. J. Maier, *Int. J. Precis. Eng. Manuf.* **2020**, *7*, 1059.

[13] R. Ramamoorthy, P. K. Dutta, S. A. Akbar, *J. Mater. Sci.* **2003**, *38*, 4271.

[14] R. Moos, K. Sahner, M. Fleischer, U. Guth, N. Barsan, U. Weimar, *Sensors* **2009**, *9*, 4323.

[15] W. C. Maskell, B. C. H. Steele, *J. Appl. Electrochem.* **1986**, *16*, 475.

[16] P. Pasierb, M. Rekas, *J. Solid State Electrochem.* **2009**, *13*, 3.

[17] L. Zhu, A. Al-Sakeeri, F. Lenrick, O. Darselius Berg, P. Sjödin, A. A. Zakharov, A. Knutsson, A. Mikkelsen, *Surf. Interface Anal.* **2022**, *54*, 99.

[18] W. Maus-Friedrichs, H. Hoermann, V. Kempter, *Surf. Sci.* **1989**, *224*, 112.

**ADVANCED
SCIENCE NEWS**

www.advancedsciencenews.com

**ADVANCED
ENGINEERING
MATERIALS**

www.aem-journal.com

[19] T.-Y. Lin, S.-K. Lee, G.-M. Huang, C.-W. Huang, K.-L. Tai, C.-Y. Huang, Y.-C. Lo, W.-W. Wu, *ACS Appl. Mater. Interfaces* **2019**, *11*, 40909.

[20] P. R. Behera, B. Bhoi, R. K. Paramguru, P. S. Mukherjee, B. K. Mishra, *Metall. Mater. Trans. B* **2019**, *50*, 262.

[21] R. K. Rains, R. H. Kadlec, *Metall. Trans.* **1970**, *1*, 1501.

[22] M. Mozetič, A. Vesel, J. Kovač, R. Zaplotnik, M. Modic, M. Balat-Pichelin, *Thin Solid Films* **2015**, *591*, 186.

[23] J. Novakovic, O. Papadopoulou, P. Vassiliou, E. Filippaki, Y. Bassiakos, *Anal. Bioanal. Chem.* **2009**, *395*, 2235.

[24] Y.-S. Lin, S.-M. Lin, J.-Y. Li, M.-C. Liao, *Soldering Surf. Mount Technol.* **2017**, *30*, 42.

[25] Y. S. Seo, A.-A. H. Mohamed, K. C. Woo, H. W. Lee, J. K. Lee, K. T. Kim, *IEEE Trans. Plasma Sci.* **2010**, *38*, 2954.

[26] M. C. Kim, D. K. Song, H. S. Shin, S.-H. Baeg, G. S. Kim, J.-H. Boo, J. G. Han, S. H. Yang, *Surf. Coat. Technol.* **2003**, *171*, 312.

[27] A. Fridman, A. Chirokov, A. Gutsol, *J. Phys. D: Appl. Phys.* **2005**, *38*, R1.

[28] U. Kogelschatz, *Plasma Chem. Plasma Process.* **2003**, *23*, 1.

[29] R. Brandenburg, *Plasma Sources Sci. Technol.* **2017**, *26*, 053001.

[30] A. Fridman, *Plasma Chemistry*, Cambridge University Press, Cambridge **2008**.

[31] Y. Sawada, N. Taguchi, K. Tachibana, *Jpn. J. Appl. Phys.* **1999**, *38*, 6506.

[32] Z. J. Xu, B. Qi, L. B. Di, *Adv. Mater. Res.* **2013**, *690–693*, 1664.

[33] L. Di, X. Zhang, Z. Xu, *Plasma Sci. Technol.* **2014**, *16*, 41.

[34] V. Udachin, L. Wegewitz, S. Dahle, W. Maus-Friedrichs, *Plasma Chem. Plasma Process.* **2022**, *42*, 1169.

[35] X. Tu, H. J. Gallon, J. C. Whitehead, *Catal. Today* **2013**, *211*, 120.

[36] V. Udachin, L. Wegewitz, S. Dahle, W. Maus-Friedrichs, *Appl. Surf. Sci.* **2022**, *573*, 151568.

[37] J. Knipping, H. Wiggers, B. Rellinghaus, P. Roth, D. Konjhodzic, C. Meier, *J. Nanosci. Nanotechnol.* **2004**, *4*, 1039.

[38] N. W. Hurst, S. J. Gentry, A. Jones, B. D. McNicol, *Catal. Rev.* **1982**, *24*, 233.

[39] T. Kim, G.-H. Cho, J.-W. Lim, *Adv. Powder Technol.* **2022**, *33*, 103729.

[40] S. Cho, T. Kim, J.-W. Lim, *ECS J. Solid State Sci. Technol.* **2022**, *11*, 045008.

[41] L. Kong, T. Ouchi, C. Zheng, T. H. Okabe, *J. Electrochem. Soc.* **2019**, *166*, E429.

[42] J. Li, Z. Hao, Y. Shu, J. He, *J. Mater. Res. Technol.* **2020**, *9*, 14792.

[43] A. M. Abdelkader, D. J. Fray, *Electrochim. Acta* **2012**, *64*, 10.

[44] Q. Xu, C. Schwandt, D. J. Fray, *Adv. Mater. Res.* **2011**, *160–162*, 1131.

[45] N. Gokon, T. Mataga, N. Kondo, T. Kodama, *Int. J. Hydrogen Energy* **2011**, *36*, 4757.

[46] W. Aman, S. Nothdurft, J. Hermsdorf, S. Kaierle, M. Szafarska, R. Gustus, W. Maus-Friedrichs, L. Overmeyer, *Procedia CIRP* **2022**, *111*, 762.

[47] R. Gustus, M. Szafarska, W. Maus-Friedrichs, *J. Vac. Sci. Technol. B* **2021**, *39*, 054204.

[48] B.-A. Behrens, S. Hübner, U. Holländer, A. Langohr, C. Pfeffer, L. Albracht, *IOP Conf. Ser.: Mater. Sci. Eng.* **2021**, *1157*, 012021.

[49] L. Albracht, S. Hübner, U. Holländer, B.-A. Behrens, in *Production at the Leading Edge of Technology* (Eds: B.-A. Behrens, A. Brosius, W.-G. Drossel, W. Hintze, S. Ihlenfeldt, P. Nyhuis), Springer International Publishing, Cham **2022**, p. 3.

[50] H. J. Maier, S. Herbst, B. Denkena, M.-A. Dittrich, F. Schaper, S. Worpenberg, R. Gustus, W. Maus-Friedrichs, *Metals* **2020**, *10*, 1161.

[51] N. Emminghaus, S. Fritsch, H. Büttner, J. August, M. Tegtmeier, M. Huse, M. Lammers, C. Hoff, J. Hermsdorf, S. Kaierle, *Adv. Ind. Manuf. Eng.* **2021**, *2*, 100040.

[52] A. S. M. Ang, N. Sanpo, M. L. Sesso, S. Y. Kim, C. C. Berndt, *J. Therm. Spray Technol.* **2013**, *22*, 1170.

[53] M. R. Diaz, M. Nicolaus, K. Möhwald, H. Maier, *Therm. Spray Bull.* **2021**, *14*, 120.

[54] M. Rodriguez Diaz, M. Szafarska, R. Gustus, K. Möhwald, H. J. Maier, *Metals* **2022**, *12*, 684.

[55] M. Rodriguez Diaz, S. Raumel, M. C. Wurz, M. Szafarska, R. Gustus, K. Möhwald, H. J. Maier, *Coatings* **2022**, *12*, 1482.

[56] V. Gourlaouen, E. Verna, P. Beaubien, *Enhanced Copper Coating Properties Obtained by Electric Wire Arc Spraying Process* ASM International **2000**, p. 685, https://doi.org/10.31399/asm.cp.itsc2000p0685.

[57] M. Mohammadpour, B. Yang, H.-P. Wang, J. Forrest, M. Poss, B. Carlson, R. Kovacevic, *Opt. Laser Technol.* **2020**, *129*, 106303.

[58] W. Reimann, S. Pfriem, T. Hammer, D. Päthe, M. Ungers, K. Dilger, *J. Mater. Process. Technol.* **2017**, *239*, 75.

[59] D. Donst, A. Janssen, M. Niessen, F. Klocke, *ICALEO* **2009**, *2009*, 440.

[60] W. Aman, S. Nothdurft, J. Hermsdorf, S. Kaierle, M. Szafarska, R. Gustus, L. Overmeyer, *J. Laser Appl.* **2022**, *34*, 022005.

[61] A. Fromm, R. Gawlytta, E. Holzmann, C. Klose, H. J. Maier, Giesserei **2022**.

[62] A. C. Fromm, K. Barienti, A. Selmanovic, S. E. Thürer, F. Nürnberger, H. J. Maier, C. Klose, Inter Metalcast **2022**.

[63] S. Raumel, K. Barienti, F. Dencker, F. Nürnberger, M. C. Wurz, *Tribol. Schmierungstech.* **2021**, *68*, 5.

[64] S. Raumel, K. Barienti, H.-T. Luu, N. Merkert, F. Dencker, F. Nürnberger, H. J. Maier, M. C. Wurz, *Friction* **2023**, https://doi.org/10.1007/s40544-022-0695-5.

[65] S. Sun, M. Brandt, M. S. Dargusch, *Int. J. Mach. Tools Manuf.* **2010**, *50*, 933.

[66] P. Müller-Hummel, M. Lahres, *Diamond Relat. Mater.* **1995**, *4*, 1216.

[67] C.-F. Wyen, K. Wegener, *CIRP Ann.* **2010**, *59*, 93.

[68] T. Grove, B. Denkena, O. Maiß, A. Krödel, H. Schwab, U. Kühn, *J. Mech. Sci. Technol.* **2018**, *32*, 4883.

[69] P. J. Arrazola, T. Özel, D. Umbrello, M. Davies, I. S. Jawahir, *CIRP Ann.* **2013**, *62*, 695.

[70] B. Denkena, M. A. Dittrich, A. Krödel, S. Worpenberg, J. Matthies, F. Schaper, *Defect Diff. Forum* **2020**, *404*, 28.

[71] Y. C. Chim, X. Z. Ding, X. T. Zeng, S. Zhang, *Thin Solid Films* **2009**, *517*, 4845.

[72] F. Schaper, B. Denkena, M.-A. Dittrich, A. Krödel, J. Matthies, S. Worpenberg, in *Production at the Leading Edge of Technology* (Eds: B.-A. Behrens, A. Brosius, W. Hintze, S. Ihlenfeldt, J.P. Wulfsberg), Springer, Berlin, Heidelberg **2021**, p. 275.

[73] V. Prasanthan, B. Denkena, B. Bergmann, *Prod. Eng. Res. Dev.* **2022**, *17*, 57.

[74] L. Albracht, B.-A. Behrens, S. Hübner, E. Farahmand, A. Langohr, U. Holländer, *wt Werkstattstech. Online* **2021**, *111*, 893.

[75] F. W. Bach, K. Möhwald, U. Holländer, *Key Eng. Mater.* **2010**, *438*, 73.

[76] K. Barienti, S. Werwein, S. Herbst, H. J. Maier, F. Nürnberger, *Manuf. Lett.* **2023**, *36*, 9.

[77] N. Emminghaus, R. Bernhard, J. Hermsdorf, S. Kaierle, *Int. J. Adv. Manuf. Technol.* **2022**, *122*, 1679.

[78] D. Lützenkirchen-Hecht, D. Wulff, R. Wagner, R. Frahm, U. Holländer, H. J. Maier, *J. Mater. Sci.* **2014**, *49*, 5454.

[79] H. D. Baehr, K. Stephan, *Wärme- Und Stoffübertragung*, Springer Vieweg, Berlin Heidelberg **2016**.

[80] C. Klose, P. Freytag, M. Otten, S. E. Thürer, H. J. Maier, *Adv. Eng. Mater.* **2018**, *20*, 1701027.

Lienhard Wegewitz received his doctorate in Physics from Clausthal University of Technology in 2015. After working as Senior Consultant in Supply Chain Management at ORSOFT, he returned to Clausthal University of Technology in 2018. He is currently working at the Clausthal Centre for Material Technology with his main research interest in the interaction of Dielectric Barrier Discharges with surfaces and the transfer of observed effects into applications. Other research interests include physicochemical interactions at polymer–metal interfaces and plasma treatment of self-assembled nanostructures.

Wolfgang Maus-Friedrichs received his doctorate in Physics from Clausthal University of Technology in 1991. From 1992 to 1994 he was head of product development at Sympatec GmbH. From 1994 to 2009 he worked as senior researcher at Clausthal University of Technology where he received his habilitation in material physics in 2004. In 2009 he was appointed adjunct professor at Clausthal University of Technology. Since 2020 he is board spokesman of the Clausthal Centre for Material Technology. His research interests include nonthermal plasma treatments of technical surfaces, surface functionalization, vacuum technology and sensor applications.

René Gustus is a research associate at the Clausthal Centre for Material Technology at Clausthal University of Technology. He studied physics and completed his PhD in surface physics in 2016. His dissertation focused on the physicochemical interactions at the polymer melt/metal interface. He is qualified in the field of surface and material analysis and is investigating physicochemical processes at surfaces and interfaces as well as the application and influence of dielectric barrier discharge plasmas on gases and surfaces.

Hans Jürgen Maier received his doctorate in Materials Science from Friedrich–Alexander University (FAU) of Erlangen-Nürnberg in 1990 and continued his engagement as a Post-Doc until 1993. He was Senior Research Engineer at the University of Siegen from 1993 to 1999, when he was appointed Chair Professor for Materials Science at the University of Paderborn. Since 2012, he is Chair Professor and Director of the Institute for Materials Science at the Leibniz University Hanover. He served inthe German Research Foundation's and the German Federation of Industrial Research Associations' Standing Review Committees. His research interests include Microstructure-Property-Relationships in Advanced Metallic Materials, Thermomechanical Fatigue Behaviour, Material Modelling, Heat Treatment and Phase Transformation.

Sebastian Herbst received his doctorate in mechanical engineering in 2018 and has since been head of the "Materials Technology" group at the Institute for Materials Science of the Leibniz University Hanover. His research focusses on thermomechanical treatment of metals ranging from conventional steels to shape memory alloys and the production, analysis and enhancement of properties of metallic hybrid materials. Since 2020 he is managing director of the collaborative research center on "Oxygen-free Production".